Technical Notes

AC/DC Current Probe CT6844/CT6845/CT6846

Kenta Ikeda
Engineering Division 6, Engineering Department 1

***Abstract*—**The AC/DC Current Probe CT6844/CT6845/CT6846 is a clamp-on current sensor with a broad frequency range that starts from DC, a broad operating temperature range, and the ability to measure currents of up to 500 A (CT6844 and CT6845) or 1 kA (CT6846). This paper describes the product's features, architecture, and characteristics.

I. Introduction

Currently, research in the field of alternative energy is focused on improving the efficiency of power conditioners that convert DC power into AC power. In addition, there is increased demand for high-accuracy clamp-on current sensors that can measure large currents, reflecting the use of larger currents by increasingly large-scale energy-saving equipment at facilities such as solar power plants (megasolar installations) and the need for instantaneous current measurement as part of anomaly testing. In the past, the Universal Clamp On CT 9279 has been used as a high-accuracy clamp-on sensor for large currents, but that product failed to offer the level of performance required in the field in terms of heat resistance and measurement reproducibility. Compared to past clamp-on current sensors, the AC/DC Current Probe CT6844/CT6845/CT6846 (with a 500 A/500 A/1 kA rating) delivers dramatic improvements in heat resistance and across-the-board performance.

II. Overview

The CT6844/CT6845/CT6846 is a successor model to the Universal Clamp On CT 9279, which Hioki launched in 1994. It offers basic measurement accuracy of ±0.3% rdg. and a measurement band that extends from DC to 200 kHz (CT6844).

Anticipating that the product would find use in a variety of environmental testing applications, Hioki gave it a broad operating temperature range of −40°C to 85°C (−40°F to 185°F). Thanks to its small size and ability to measure currents of up to 500 A, the CT6844 is ideal for measuring large currents in hot, confined spaces such as vehicle engine compartments. Since they can be applied to conductors that measure up to 50 mm in diameter, the CT6845 and CT6846 can be used to quickly measure multi-cable circuits consisting of thick cables or high-current lines. The sensors' jaw design has been significantly improved from that of legacy products to minimize effects that specifically affect clamp-on current sensors (conductor position, external magnetic fields, and magnetization), enabling highly reproducible measurement.

Appearance of the CT6844.

Appearance of the CT6845.

III. Features

A. High-accuracy Broadband Measurement of Large Currents With a Clamp-on Sensor

The sensors' newly developed clamp-on core offers high accuracy of ±0.3% rdg. and a measurement band that extends up to a maximum of 200 kHz (CT6844) with a high current rating of 500 A or 1 kA. Thanks to excellent phase accuracy characteristics of ±0.1°, these sensors can also be used with a power meter to measure power.

B. Broad Operating Temperature Range of −40°C to 85°C (−40°F to 185°F)

Thanks to their adoption of a construction that utilizes highly heat-resistant parts, a core material that exhibits

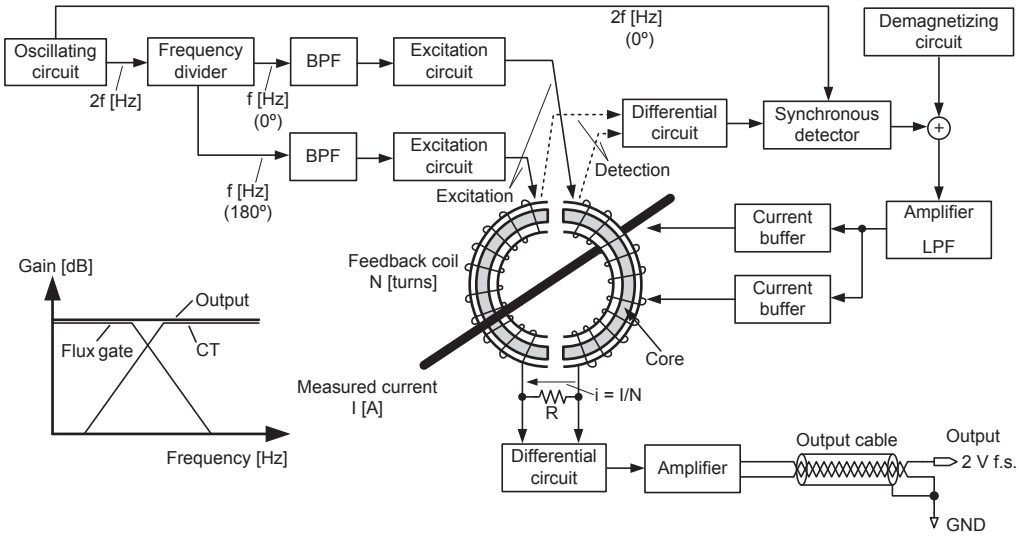

Fig. 1. Circuit architecture.

minimal deterioration of characteristics under conditions of high heat, and a design that maximizes the dissipation of heat from heat-generating circuit board components, the sensors deliver stable characteristics across a broad operating temperature range that extends from −40°C to 85°C (−40°F to 185°F).

C. *Defined Amplitude and Phase Accuracy Across the Entire Measurement Band*

Generally speaking, the amplitude accuracy of most current sensors used in combination with power meters is only defined for DC and commercial frequencies (50 Hz and 60 Hz), while phase accuracy is not defined at all.

By contrast, amplitude and phase accuracy, both of which are important in power measurement, have been defined for the CT6844/CT6845/CT6846 across the entire measurement band. Furthermore, these accuracy figures can be calibrated for any frequency that falls within the measurement band.

D. *Minimization of Current Sensor-specific Effects*

Thanks to the sensor core's laterally symmetrical construction, the impact of the effects that specifically affect clamp-on current sensors (conductor position, external magnetic fields, and magnetization) has been minimized compared to legacy products. Despite their clamp-on design, these sensors deliver performance that approaches that of pass-through current sensors, enabling highly reproducible measurement.

E. *Lock Mechanism Designed to Endure Vibration and Mechanical Shocks*

The sensor unit of legacy products was prone to snap open if the instrument was subjected to vibration or mechanical shocks during measurement. The CT6844/CT6845/CT6846's sensor unit incorporates a lock mechanism, eliminating concerns that the sensor unit will snap open during measurement.

IV. Architecture and Construction

A. *Circuit Architecture*

Fig. 1 illustrates the sensors' circuit architecture. These zero-flux DC sensors combine flux gate and current transformer (CT) detection to deliver a measurement band that extends from DC to AC frequencies.

Flux gate detection, a type of magnetic detection that takes advantage of the nonlinear nature of a magnetic material's B-H characteristics, is also used to detect minuscule magnetic fields such as terrestrial magnetism. Compared to detection methods that use semiconductors such as Hall elements, which are widely known, flux gate detection offers a low offset voltage along with excellent temperature stability and long-term stability.

For the CT6844/CT6845/CT6846, a pair of flux gate coils is incorporated into the magnetic core. The coils are excited by a current (with a frequency f of 1.65 MHz) such that the magnetic flux density they generate reaches the level of saturation. When an external magnetic field is applied under these conditions, a different voltage waveform is generated at the end of each of the flux gate coils. The differential signal obtained from those waveforms has a frequency component that is twice that of the exciting current. Consequently, a signal that is proportional to the current under measurement can be obtained by performing synchronous detection using a 2f (3.3 MHz) signal that is synchronized with the excitation signal.

However, because saturation of the magnetic material hampers the sensitivity of the flux gate method when used alone to detect a strong magnetic field, the new sensors

utilize zero-flux detection. Since this design incorporates a negative feedback circuit that includes the magnetic circuit, operating magnetic flux can be kept to an extremely low level. Consequently, the effects of the nonlinearity of the magnetic material can be minimized, allowing the CT6846 to exhibit linearity for DC currents of up to 1.7 kA.

B. Construction

Figs. 2 and 3 illustrate the sensors' construction, while TABLE I provides a comparison of the construction of the sensor unit with that of the 9279 (a legacy model).

The CT6844 utilizes the enclosure of the CT6841/CT6843 (legacy models), and the principal focus in designing the new instruments was on reducing their size. A sliding mechanism that opens and closes the jaws and a lock mechanism allow the user to open, close, and lock the instrument with a series of simple movements that can be performed singled-handedly.

The CT6845/CT6846 is larger, but Hioki still focused on usability in order to engineer a design that allows single-handed opening, closing, and locking of the mechanism. Both utilize a robust lock mechanism to ensure that the jaws will not easily become unlocked if the instrument is subjected to mechanical shock during measurement.

The position of the flux gate coils inside the sensor unit and the design of the feedback winding have been significantly changed from legacy products so that the sensor cores are laterally symmetrical in the manner of a pass-through sensor, minimizing the impact of various effects on measurement.

C. Consideration of Components' Heat Resistance

TABLE II compares the components used in these sensors with those used in the 9279 (a legacy model). The increase in the sensors' operating temperature range posed issues in terms of the heat generated by components and the characteristics of the magnetic material used in the core. Because the ferrite material used for the 9279's core has a comparatively low Curie temperature, which causes a degradation in its characteristics in the vicinity of 100°C (212°F) due to the resulting reduction in magnetic permeability, Hioki chose a permalloy material with a Curie temperature higher than that of ferrite material for the new sensors. In addition, recognizing that the temperature inside the enclosure would rise due to heat generated by internal circuitry, the company chose electrical components with greater heat resistance than legacy products and designed the instrument so that heat from heat-producing components would be dissipated to the shield.

In addition, Hioki chose a polycarbonate material with high heat resistance for the enclosure and added glass fiber to increase its mechanical strength.

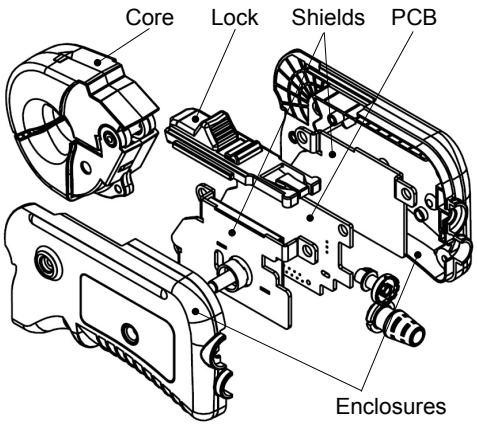

Fig. 2. CT6844 construction.

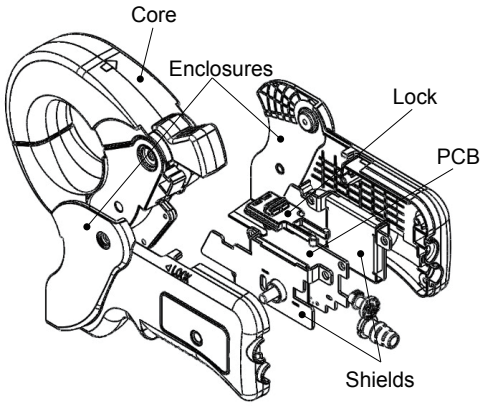

Fig. 3. CT6845/CT6846 construction.

TABLE I. Comparison of Sensor Unit With Legacy Product

	9279	CT6844/CT6845/CT6846
Main core	Ferrite (Permeability: Approx. 5000)	Permalloy (PC) (Permeability: Approx. 60000)
Jaw mating surface	Flat surface	Interlocking teeth
Flux gate position	2 on one side of core	1 on each side of core
Feedback winding construction	Concentrated winding	Level winding

TABLE II. Comparison of Component Heat Resistance With Legacy Product

	9279	CT6844/CT6845/CT6846
Electrical component heat resistance	85°C (185°F)	125°C (257°F)
Cable heat resistance	80°C (176°F)	105°C (221°F)
Outer resin material	ABS	Polycarbonate (With glass fibers)

V. Reference Characteristics Data (standalone use)

(Used in combination with the Sensor Unit 9555-10)

A. Linearity

Figs. 4 through 6 illustrate the sensors' linearity. All three products exhibit excellent linearity that exceeds the

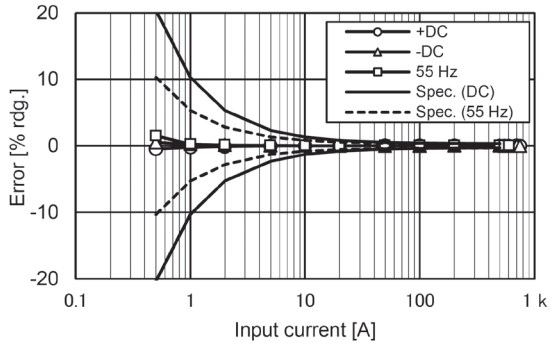

Overall

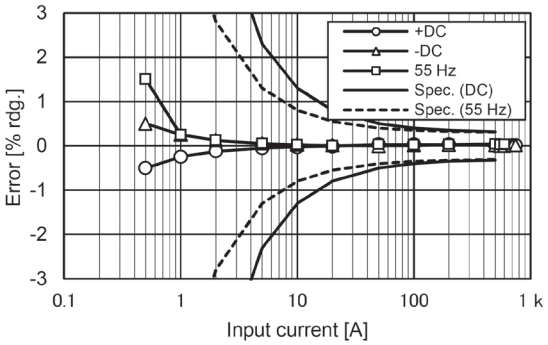

Enlarged view

Fig. 4. CT6844 linearity.

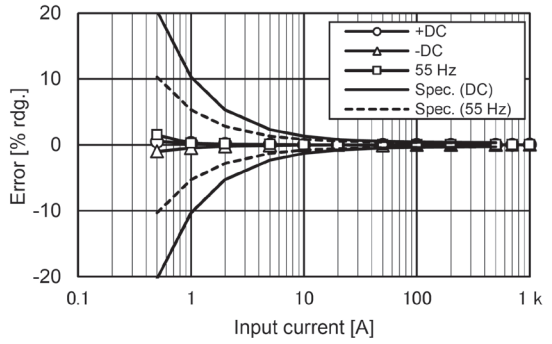

Overall

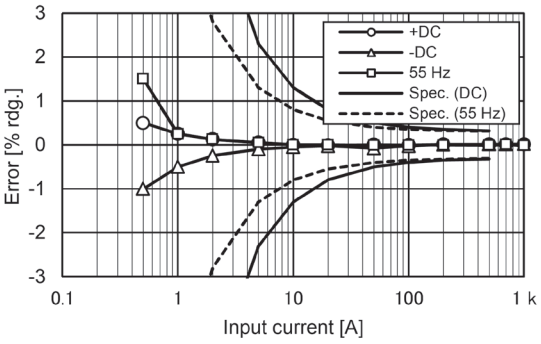

Enlarged view

Fig. 5. CT6845 linearity.

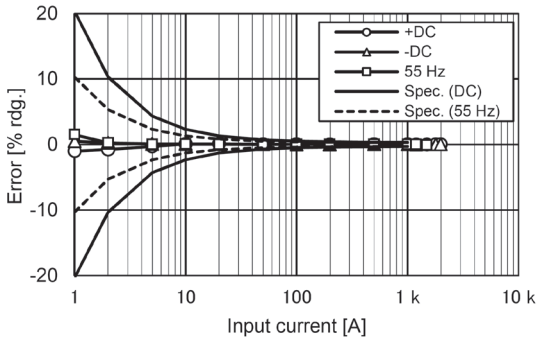

Overall

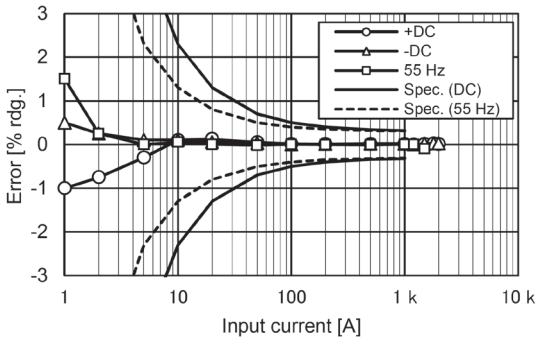

Enlarged view

Fig. 6. CT6846 linearity.

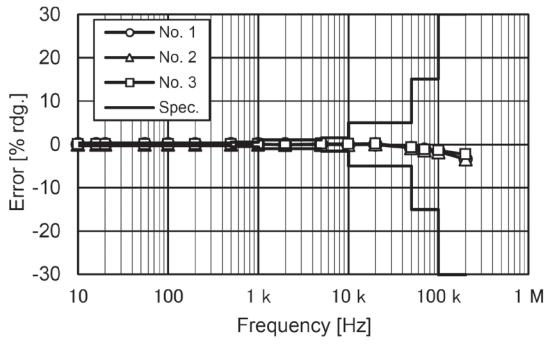

Overall

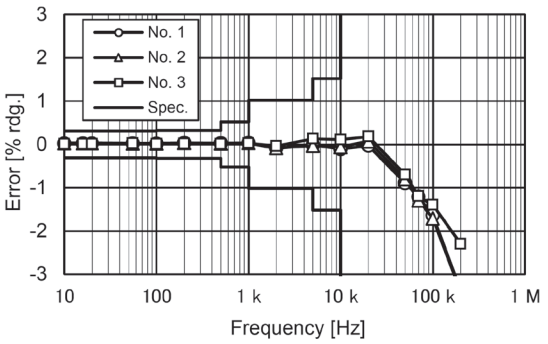

Enlarged view

Fig. 7. CT6844 amplitude-frequency characteristics.

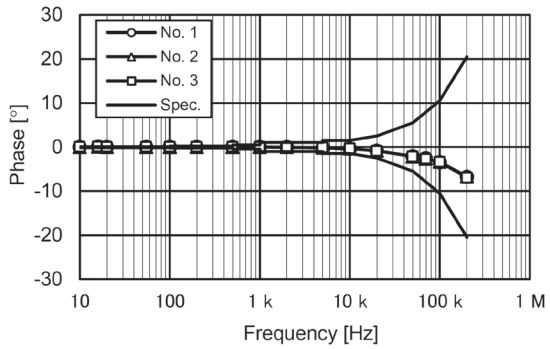

Overall

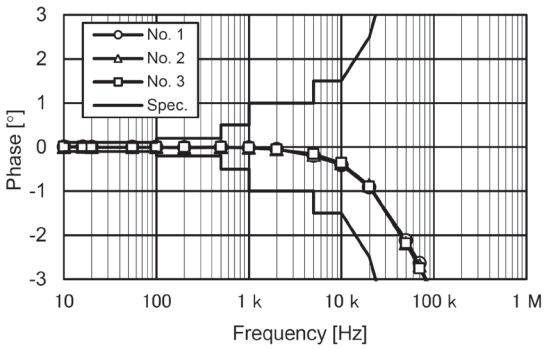

Enlarged view

Fig. 8. CT6844 phase-frequency characteristics.

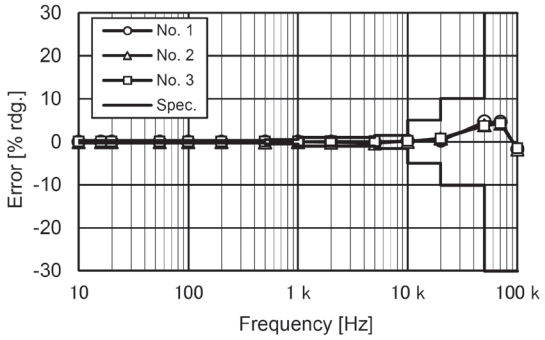

Overall

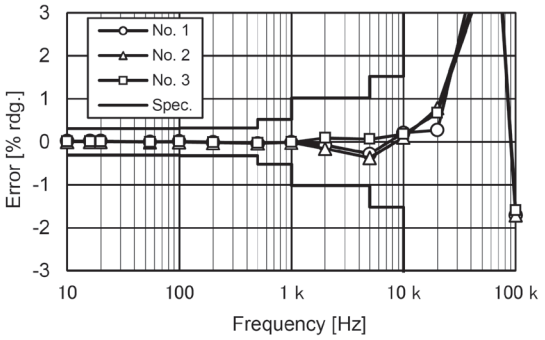

Enlarged view

Fig. 9. CT6845 amplitude-frequency characteristics.

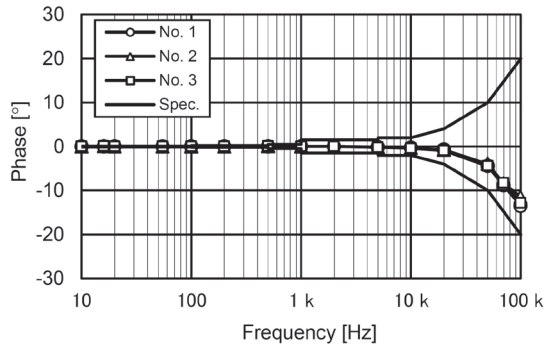

Overall

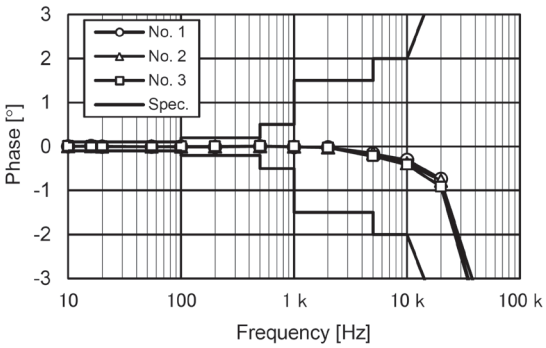

Enlarged view

Fig. 10. CT6845 phase-frequency characteristics.

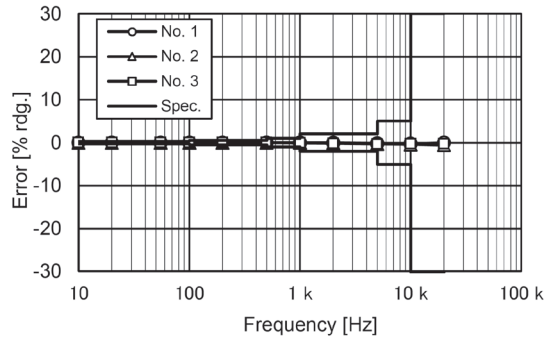

Overall

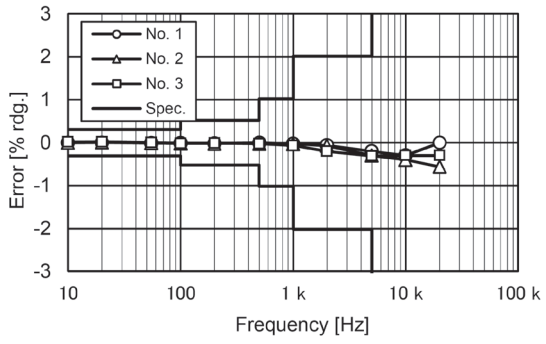

Enlarged view

Fig. 11. CT6846 amplitude-frequency characteristics.

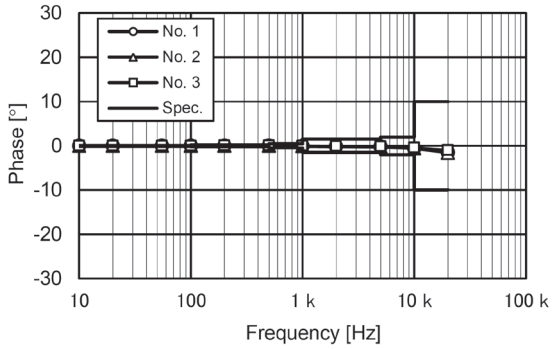

Overall

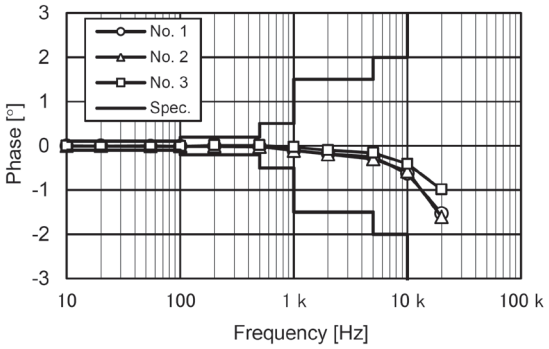

Enlarged view

Fig. 12. CT6846 phase-frequency characteristics.

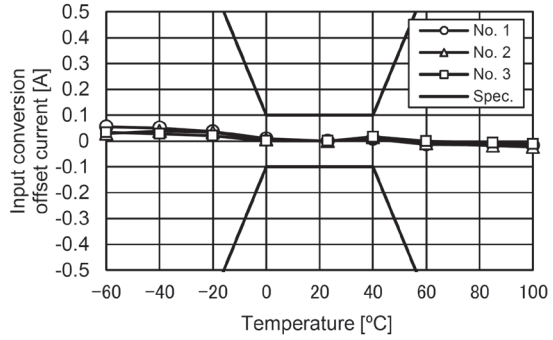

Offset

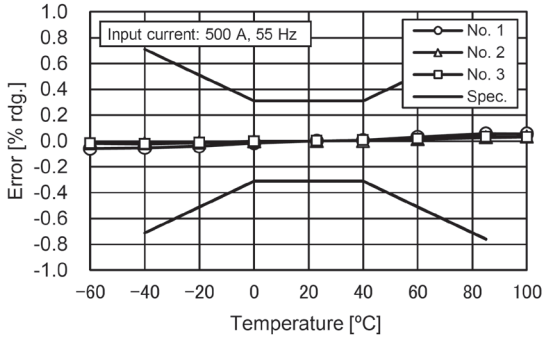

Sensitivity

Fig. 13. CT6844 temperature characteristics.

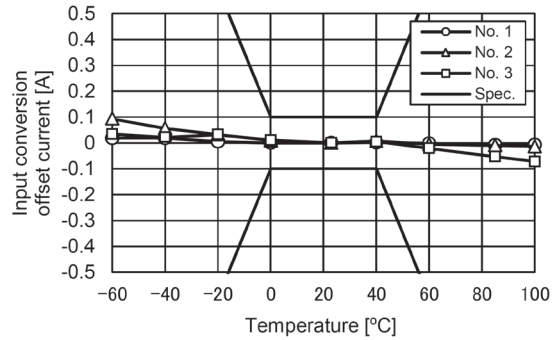

Offset

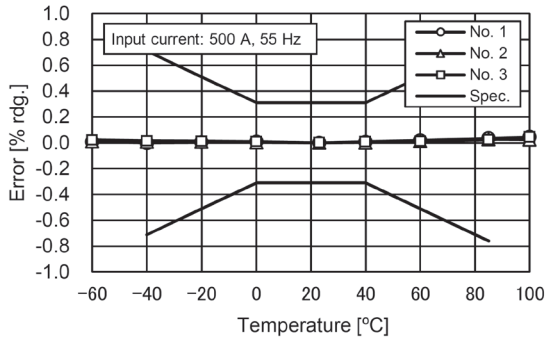

Sensitivity

Fig. 14. CT6845 temperature characteristics.

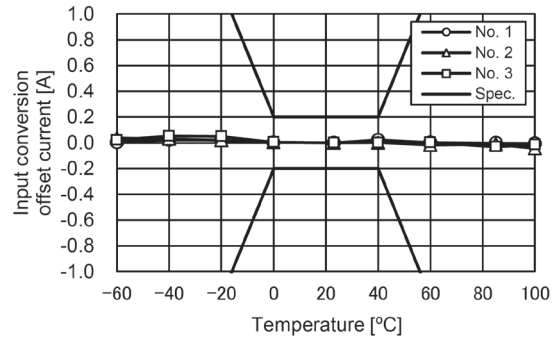

Offset

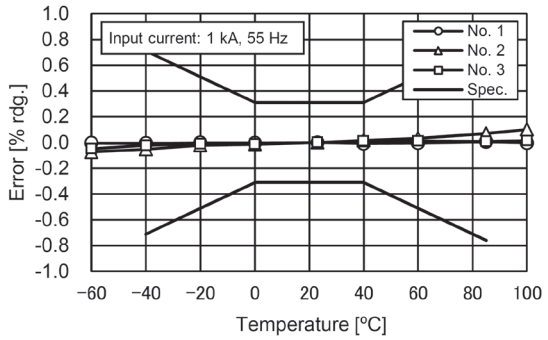

Sensitivity

Fig. 15. CT6846 temperature characteristics.

rated current over a broad range. Pre-measurement offset adjustment makes it possible to measure even low-level DC currents with a high degree of accuracy.

B. Frequency Characteristics

Figs. 7 through 12 illustrate the sensors' frequency (amplitude and phase) characteristics. These characteristics apply when the current line is positioned at the center of the sensor. A curve that remains flat up to 10 kHz indicates that the sensors are adequate for use when measuring the secondary side of a typical inverter.

C. Temperature Characteristics

Figs. 13 through 15 illustrate the sensors' temperature (offset and sensitivity) characteristics. These characteristics are extremely stable from −60°C to 100°C (−76°F to 212°F), both of which values fall outside the operating temperature range. This level of performance is sufficiently robust that the temperature coefficient defined in the specifications can be ignored. Thanks to the sensors' use of flux gate detection, they exhibit much greater temperature stability than standard current sensors that use Hall elements.

In addition, the extremely low level of variation caused by self-heating makes a pre-use warm-up period unnecessary.

D. Effects of Conductor Position

Fig. 16 illustrates the effect of conductor position while measuring a 100 A current at 55 Hz. The magnitude of the effect is much smaller than with legacy products, allowing highly reproducible measurement. The sensor unit's construction plays a dominant role in determining how much conductor position affects measurement. Hioki's decision to make significant changes to flux gate position and the design of the feedback winding, which was motivated by a desire to give the newly developed core lateral symmetry, have minimized the magnitude of this effect.

Fig. 17 illustrates the difference between maximum and minimum output when the measurement frequency and conductor position are varied. The effect at frequencies of 1 kHz and lower is extremely small. Since the effect increases above 1 kHz, it is necessary to position the conductor being measured at the center of the sensor in order to allow reproducible measurement.

E. Effects of Nearby Conductors

Fig. 18 illustrates the effect of a rated current (55 Hz) located in close proximity to each sensor. The magnitude of the effect, which remains extremely small, does not change as the conductor approaches the sensor (an issue that affected legacy products), allowing measurement that is free from the effects of nearby wiring. Since the symmetrical core design allows magnetic field components from external sources to be negated inside the core, this effect is reduced.

Fig. 19 illustrates the effect of the frequency of a nearby conductor. The graph illustrates the maximum value that occurs when the conductor is routed around the core's outer periphery, and the magnitude of the effect increases with the frequency. In environments where a high-frequency current at 1 kHz or greater is located in close proximity to the sensor, it is desirable to keep the sensor away from such wiring.

F. Effects of Magnetization

Fig. 20 illustrates the effect of magnetization. This quantity manifests itself as the offset error that occurs when the sensor core becomes magnetized after measuring a DC current. Because the amount of magnetization, and thus the magnitude of the effect on measurement, varies with the strength of the input current, this effect becomes a large source of error when measuring a minuscule current after measuring a large current. Compared to legacy products, the amount of magnetization is extremely low.

After measuring a large-current, the effects of magnetization can be canceled out by pressing the DEMAG button on the sensor to degauss the device.

G. Effects of Common-mode Voltage

Fig. 21 illustrates the effect of common-mode voltage. The graph shows sensor output values when a 1000 V rms line carrying no current is passed through the sensor. At low frequencies, there is almost no effect. Compared to legacy products, the magnitude of the effect at frequencies of 10 kHz and greater has been significantly reduced. At the voltage levels associated with standard inverter-equipped devices, this effect poses no issue.

VI. Characteristics Data When Used in Combination With a Power Meter

The following sections describe the sensors' characteristics when used in combination with a typical Power Analyzer, Hioki's PW6001. The PW6001's current inputs are designed specifically to accept input from a current sensor. This power meter takes full advantage of each sensor's performance, and no adjustment is required in order to use the instruments together. Since the power meter automatically detects the sensor and configures the range setting appropriately when the sensor is connected, no manual configuration is needed.

CT6844/CT6845 combination current ranges

(10 A/20 A/50 A/100 A/200 A/500 A)

CT6846 combination current ranges

(20 A/40 A/100 A/200 A/400 A/1 kA)

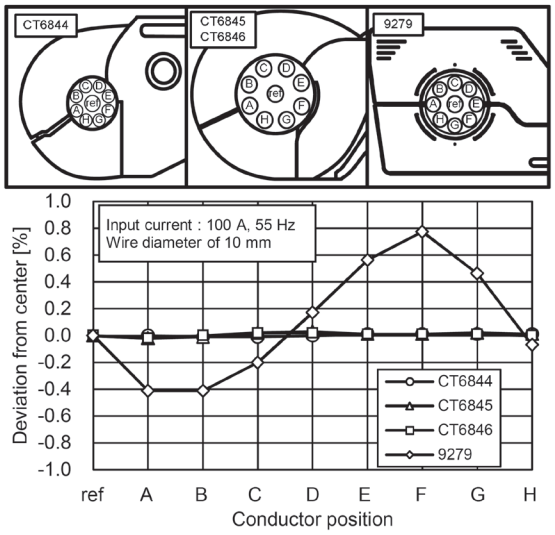

Fig. 16. Effects of conductor position (comparison with legacy product).

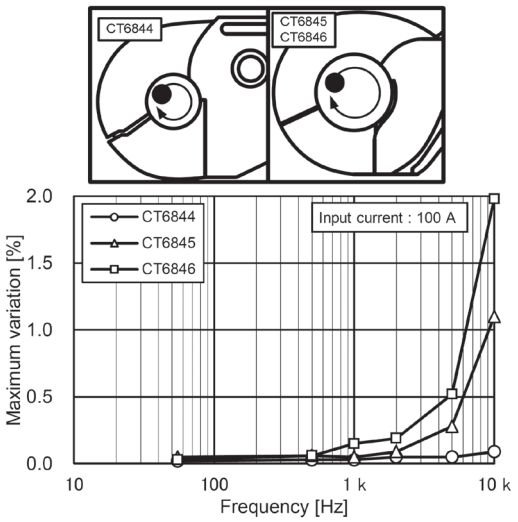

Fig. 17. Effects of conductor position by frequency.

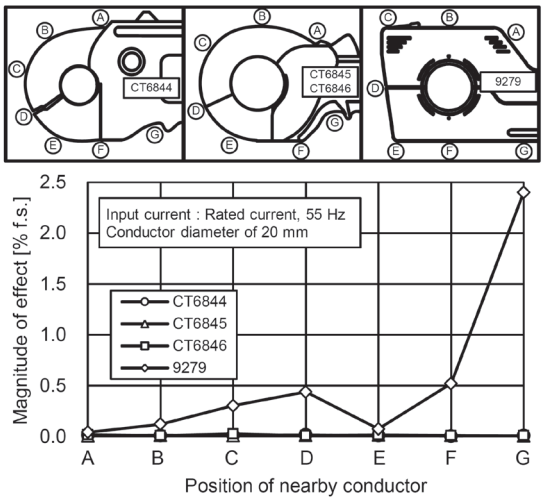

Fig. 18. Effects of position of nearby conductor (comparison with legacy product).

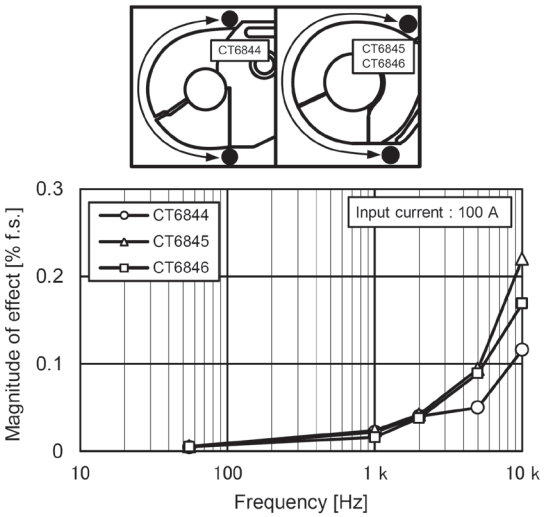

Fig. 19. Effects of nearby conductor by frequency.

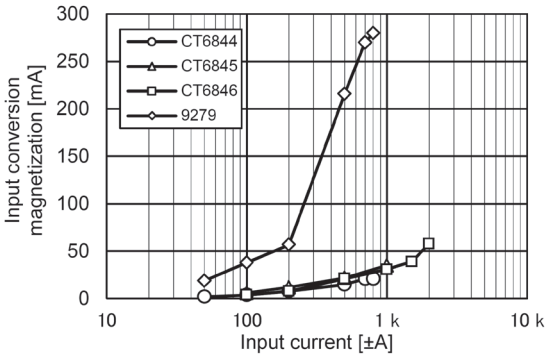

Fig. 20. Effects of magnetization.

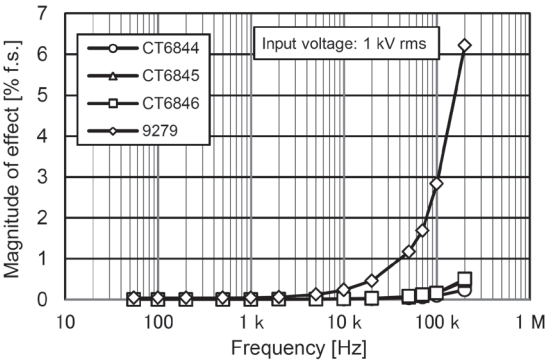

Fig. 21. Effects of common-mode voltage.

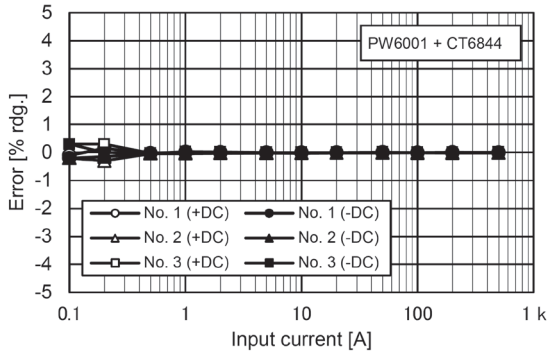

Fig. 22. DC current linearity (auto range).

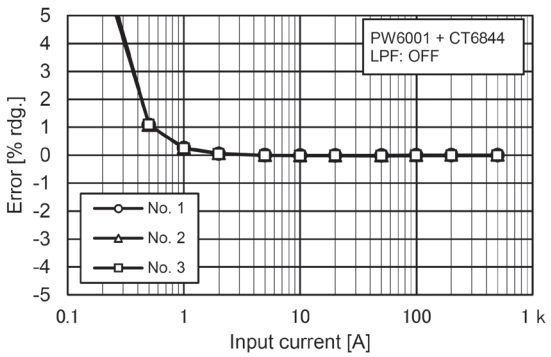

Fig. 23. AC current (55 Hz) linearity (auto range).

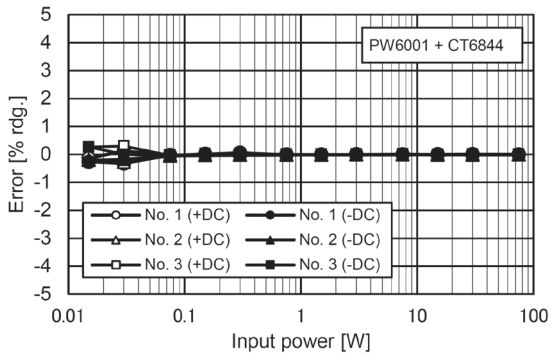

Fig. 24. DC power linearity (auto range)
voltage (+150 V fixed), current (±0.1 A to ±500 A).

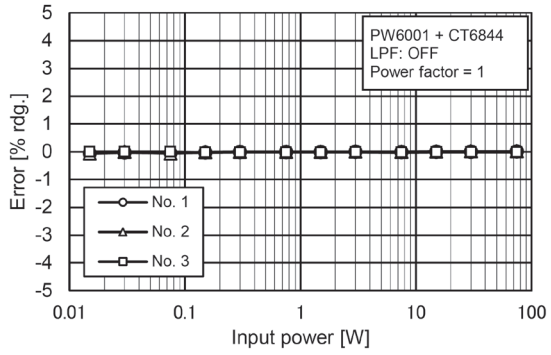

Fig. 25. AC power (55 Hz) linearity (auto range)
voltage (150 V fixed), current (0.1 A to 500 A), power factor of 1.

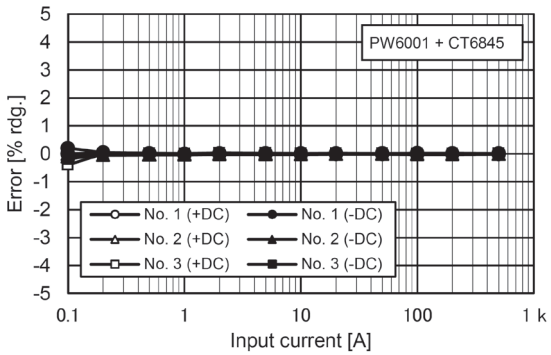

Fig. 26. DC current linearity (auto range).

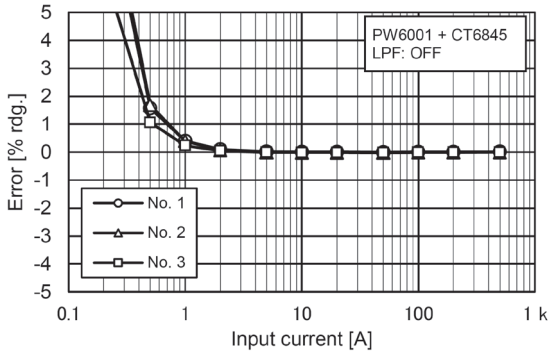

Fig. 27. AC current (55 Hz) linearity (auto range).

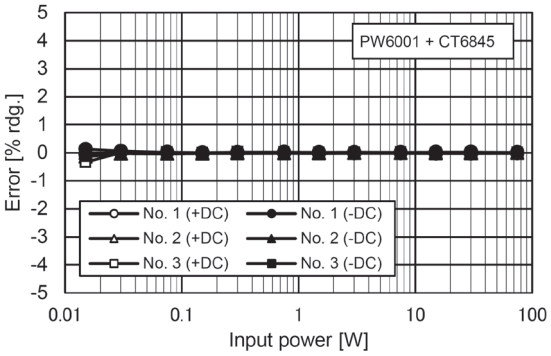

Fig. 28. DC power linearity (auto range)
voltage (+150 V fixed), current (±0.1 A to ±500 A).

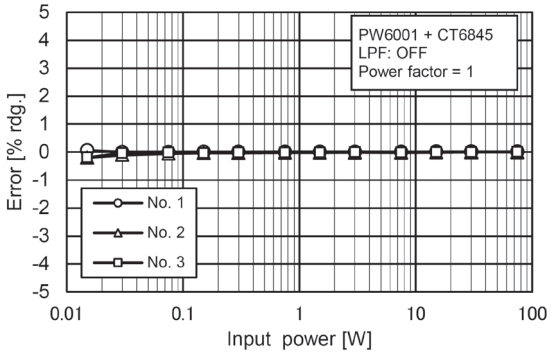

Fig. 29. AC power (55 Hz) linearity (auto range)
voltage (150 V fixed), current (0.1 A to 500 A), power factor of 1.

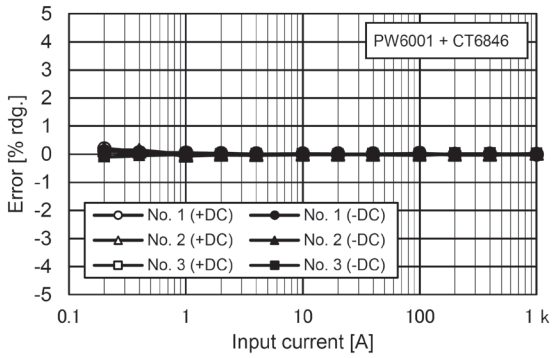

Fig. 30. DC current linearity (auto range).

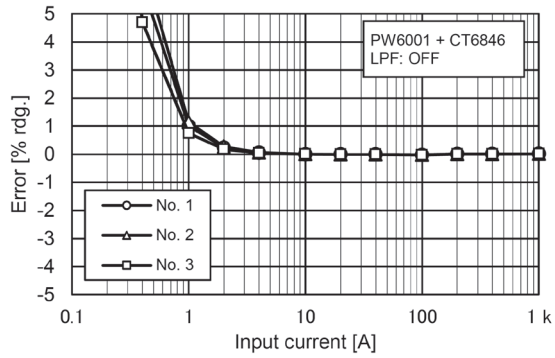

Fig. 31. AC current (55 Hz) linearity (auto range).

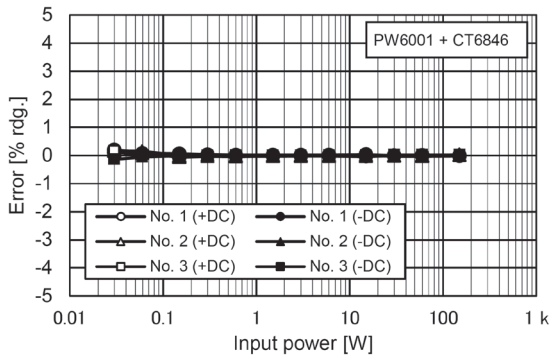

Fig. 32. DC power linearity (auto range)
voltage (+150 V fixed), current (±0.2 A to ±1 kA).

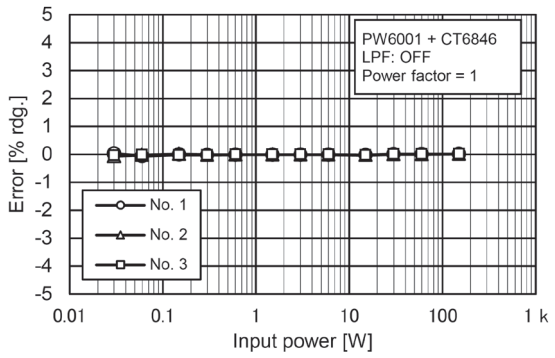

Fig. 33. AC power (55 Hz) linearity (auto range)
voltage (150 V fixed), current (0.2 A to 1 kA), power factor of 1.

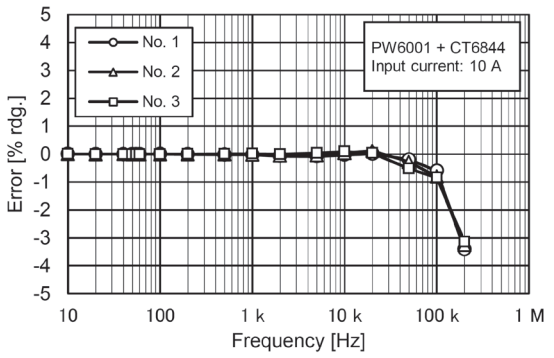

Fig. 34. PW6001 + CT6844 current frequency characteristics.

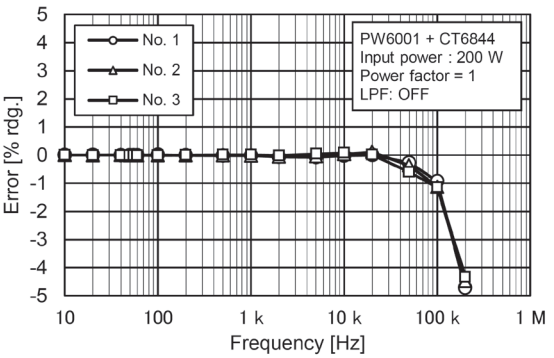

Fig. 35. PW6001 + CT6844 power frequency characteristics.

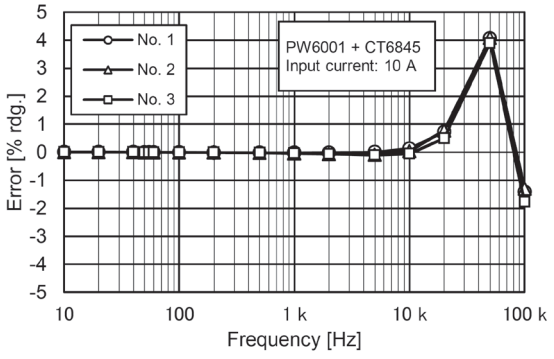

Fig. 36. PW6001 + CT6845 current frequency characteristics.

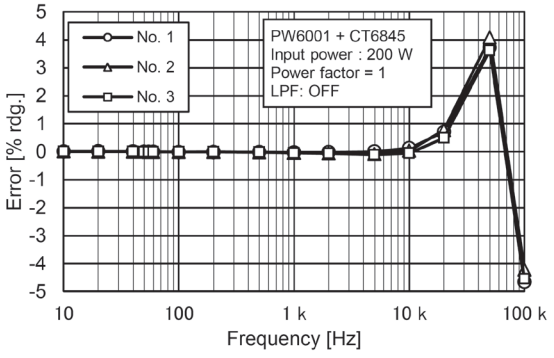

Fig. 37. PW6001 + CT6845 power frequency characteristics.

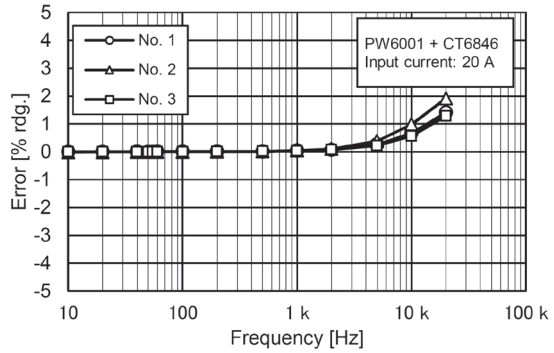

Fig. 38. PW6001 + CT6846 current frequency characteristics.

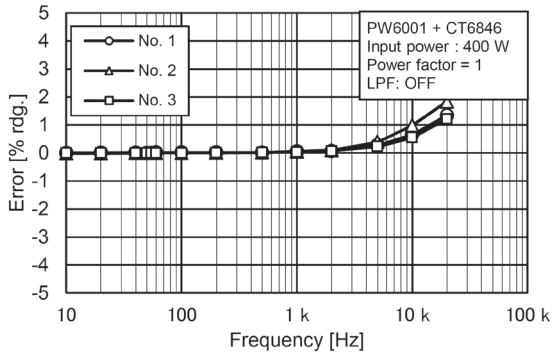

Fig. 39. PW6001 + CT6846 power frequency characteristics.

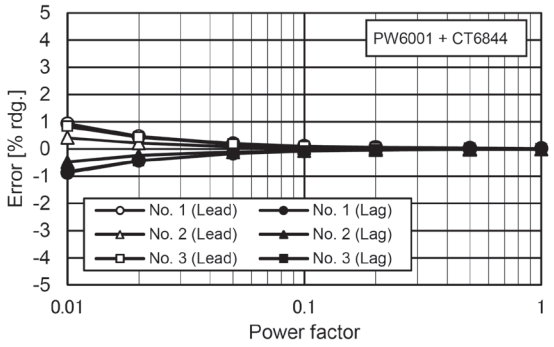

Fig. 40. Effects of power factor (150 V × 500 A, 55 Hz).

A. *Linearity*

Figs. 22 through 25 illustrate linearity when the PW6001 is used in combination with the CT6844; Figs. 26 through 29, with the CT6845; and Figs. 30 through 33, with the CT6846. Since the PW6001's zero-adjustment function can be used prior to measuring a DC current in order to cancel out the sensor's minuscule internal offset, even small currents can be measured with a high degree of accuracy. While the sensor's noise becomes dominant when measuring low (1 A or lower) AC currents, causing the current measurement precision to fall, this loss of precision does not affect power calculations, so power can nonetheless be measured with a high degree of precision. By configuring the PW6001's filter

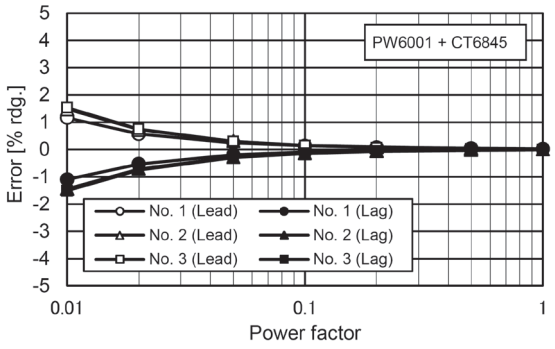

Fig. 41. Effects of power factor (150 V × 500 A, 55 Hz).

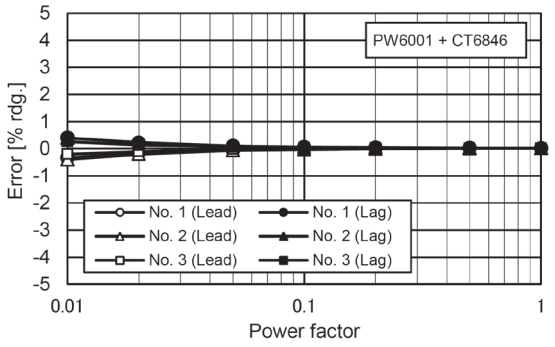

Fig. 42. Effects of power factor (150 V × 1 kA, 55 Hz).

based on the measurement frequency, even small currents can be measured with a high degree of precision.

B. *Frequency Characteristics*

Figs. 34 and 35 illustrate the frequency characteristics when the PW6001 is used in combination with the CT6844; Figs. 36 and 37, with the CT6845; and Figs. 38 and 39, with the CT6846. The characteristics exhibit excellent flatness up to 10 kHz, and there is no significant different relative to the sensors' standalone frequency characteristics.

C. *Effects of Power Factor*

Fig. 40 illustrates the effect of power factor (at 55 Hz) when the PW6001 is used in combination with the CT6844; Fig. 41, with the CT6845; and Fig. 42, with the CT6846. Phase accuracy of ±0.1° (at 55 Hz) means the sensors exhibit excellent characteristics even when measuring power at low power factors.

A deterioration in the sensor's phase characteristics causes the error component to increase when measuring high-frequency power at low power factors. By using the PW6001's phase correction function, it is possible to compensate for the sensor's phase rotation, allowing power to be measured with a high degree of accuracy even at low power factors.

VII. Conclusion

The CT6844/CT6845/CT6846 is a clamp-on current sensor that can measure currents of up to 1 kA at a significantly higher level of performance than legacy products. These sensors can be used in applications ranging from simple current measurement to development and evaluation of high-efficiency devices and energy devices, in which case they can be used in combination with a high-precision power meter. An expanded operating temperature range allows them to contribute to current measurement in a variety of types of environmental testing.

Kimihiko Yamagishi[1], Hideo Watanabe[2],
Tetsuya Komiyama[2]

References

[1] K. Yamagishi, "AC/DC Current Sensor CT6862/CT6863," *Hioki Giho*, vol. 31, no. 1, pp. 25-34, 2010. (Japanese).

[2] K. Ikeda, "AC/DC Current Probe CT6841/CT6843," *Hioki Giho* (*Hioki Technical Notes*), vol. 36, no. 1, pp. 45-54, 2015. (Japanese, also available in English).

[1] Engineering Division 6, Engineering Department 1
[2] Engineering Division 10, Engineering Department 4